SWS IN-FLIGHT CALIBRATION

R. F. Shipman[1], P. W. Morris[2], D. A. Beintema[1], D. R. Boxhoorn[4], H. Feuchtgruber[3], A. M. Heras[7], R. Huygen[5], D. J. M. Kester[1], F. Lahuis[1], K. Leech[6], R. Lorente[6], D. Lutz[3], P. R. Roelfsema[1], A. Salama[6], S. G. Schaeidt[3], E. A. Valentijn[4], B. Vandenbussche[5] and E. Wieprecht[3]

[1]Space Research Organisation of the Netherlands, Postbus 800, NL-9700 AV, Groningen, The Netherlands
[2]California Institute of Technology , 1200 E. California Blvd. Pasadena CA 91125, USA
[3]Max Planck Institut fuer extraterrestrische Physik, Giessenbachstrasse 1, D-85748 Garching, Germany
[4]Kapteyn Astronomical Institute, Postbus 800, NL-9700 AV, Groningen, The Netherlands
[5]Katholieke Universiteit Leuven, Instituut voor Sterrenkunde, Celestijnenlaan 200 B, B-3001 Heverlee, Belgium
[6]ISO Data Centre, European Space Agency, Villafranca del Castillo, P.O. Box 50727, 28080 Madrid, Spain
[7]European Space Agency - Astrophysics Division, Keplerlaan 1, NL-2201 AZ Noordwijk, The Netherlands

ABSTRACT

The calibration of the Short Wavelength Spectrometer on ISO developed significantly throughout ISO's mission and well into the Post Operations phase. The guiding principles, however, were laid down in the In-Orbit Calibration Document (IOCD) before the launch of ISO. This document specified the essential calibration procedures for SWS and aided greatly the success of the SWS instrument.

Within the framework of the IOCD, the SWS calibration and processing were allowed to remain flexible and could adjust to AOT logic changes, model updates and changes in the calibration methods used in the Post Mission phase. The result is that the final accuracies surpass pre-launch requirements.

During the mission a number of expected and unexpected issues arose. The majority of these have been addressed either as changes to observation strategies or as changes in data reduction. Some issues, like memory effects, were purely instrumental and dealt with entirely in the Post Operations Phase. There are other problems, however, which have been identified but have, as yet, no correction in the SWS calibration and processing. These issues form the caveats to the SWS data products.

Key words: SWS – calibration

1. INTRODUCTION

The calibration of the Short Wavelength Spectrometer (SWS) has been an active effort throughout the ISO mission and post operations. The goal of this article is to present the state of the grating calibration at the end of the Post Operations Phase of ISO. Presented in this article are changes to the SWS processing, updates to model SEDs for photometric standards, the list of standards used, photometric accuracies of OLP 10 products and a brief discussion of remaining issues.

A further goal of this article is to provide pointers to the wealth of information in reports and studies which are publicly available. These technical reports comprise the SWS Explanatory Library hosted at the ISO Data Centre.

The photometric calibration of the Fabry Pérots is discussed in the SWS Handbook and not presented in this article. See the Explanatory Library for further information.

2. THE SWS WAVELENGTH CALIBRATION

The wavelength calibration and resolution are well understood and characterised. Valentijn et al. (1996) present an overview of the wavelength calibration and accuracies for both the gratings and the Fabry Pérots. Two technical notes, Lutz et al. (1999) and Lorente (1998), report on the resolution of the gratings and Fabry Pérots. Kester et al. (1998) describe further updates to the wavelength calibration during the ISO mission.

3. THE SWS PHOTOMETRIC CALIBRATION

The photometric calibration is applied to each AOT band (Astronomical Observing Template). An AOT band signifies a given wavelength range which is determined by a specific combination of detector type, aperture and order. The grating detector types (InSb, Si:Ga, Si:As, Ge:Be) are separated into 4 blocks of 12 detectors each (de Graauw et al. 1996).

Schaeidt et al. (1996) give a good overview of the photometric calibration early in the ISO mission. However, the photometric calibration developed greatly throughout the mission and post operations as more objects became available and trend studies could be performed. A compilation of some of the trend studies may be found in Heras et al. (2000). A few of the trend analyses developed into modifications of the SWS processing and are discussed below.

3.1. Internal Photometric Calibration

Internal photometric calibration measurements (applied to Bands 2 to 6) were made as a standard part of every SWS science observation. Barring any losses in telemetry, these photometric calibration scans were made in every observation. The scan consisted of observing an internal stimulator with the SWS shutter closed and stepping both the long and the short wavelength gratings through 22 different positions.

One of the updates to the SWS processing for OLP 10 is to treat the internal calibration scan as an entire block of data

(12 detectors per block over 22 grating scan steps) instead of 12 separate scans. From this block of data a single photometric gain is calculated for each detector block in the observation (Shipman & Lahuis 2000).

This approach gives qualitatively the same results as earlier processing but with the significantly more stable gain values. Since the gain is calculated per detector block, a radiation hit will not have the same impact on the gain calculation as for a single detector. This modification also allows for a better estimation of the uncertainty introduced in the photometry.

3.2. Flat-Fielding

In the SWS grating scans, a spectral segment is observed with 12 separate detectors at any one time. In general, these detectors must be individually calibrated such that the resulting spectra from each detector within an AOT band give the same signal.

In the In-Orbit Calibration Document (IOCD, Valentijn 1995), it was recognised that the signal-to-flux calibration per detector formally takes care of the flat-fielding. However, the responsivity of an individual detector relative to the average of the 12 detectors is quite stable and can be determined from a large number of observations (1000 were used). Therefore, an independent flat-fielding measure was introduced into the pipeline to bring the response of each detector in agreement with the average of all the detectors within an AOT band (Shipman 2000).

Although flat-fielding is usually performed entirely in post processing, the application of a separate flat-fielding step aids in removing some of the ambiguity of applying either a scaling or an offset correction. As treated in the standard processing, the flat-fielding is always a scaling correction. In post processing it still might be necessary to account for offsets introduced through the dark current application. There remain cases when it is still preferred to apply a flat-fielding correction in post processing; however, the correction will be smaller.

3.3. Memory Effects

An SWS grating scan consists of two scans over a spectral segment within an AOT band. Memory effects manifest themselves as a difference between the 1st (Up) and 2nd (Down) scans of the same spectral range. In OLP 10, a 1st order correction based on the Fouks-Schubert model (Fouks & Shubert 1995) is applied to the band 2 (Si:Ga) detectors. A full description of the SWS application and validation of the memory model can be found in Kester (2001).

Errors listed in Table 2 include the influence of the residual memory effects. Large signal steps (few thousand μV/sec) introduce a short lived higher order memory term. This higher order effect is not accounted for by the memory model used in SWS processing.

Figure 2 shows the influence of the residual memory in the first and second scan of two bright stellar sources. The difference between the UP and the DOWN scan is especially noticeable in AOT band 2A (4-5.3 μm) where the higher order memory term is especially strong.

Although band 4 (Ge:Be) is also affected by memory effects, there is no theoretical model for these effects and no pipeline correction is applied.

4. SWS ASTRONOMICAL CALIBRATION SOURCES

A full description of the SWS Astronomical Calibration Sources (ACS) can be found in Schaeidt et al. (1996) and references therein. Table 1 gives an overview of the ACSs used for the photometric calibration of the OLP 10 products. The table indicates the source name, type of object, and AOT band which made use of the ACS.

The last column illustrates the diversity and distribution of observations used for the photometric calibration of the various AOT bands. For each ACS, the number of observations going into the photometric calibration is given. In the last column, there are 4 numbers per ACS indicating 4 different band groups. The first group combines AOT bands 1A through 2C and the second group combines AOT bands 3A through 3D. The last two groups are the AOT bands 3E and 4 respectively.

For wavelengths shorter than 12 μm, the SEDs for the ACS were updated with stellar atmospheric models described in Decin (2000). The absolute calibration of these SEDs is based on the photometry used for the absolutely calibrated composite observed spectra described by Cohen et al. (1992b, 1995, 1996). For wavelengths longer that 12 μm the stellar composites themselves are used (Cohen et al. 1992b, 1995, 1996). The photometry and composites used for SWS are directly traceable to the published calibrated spectra of Sirius and Vega (Cohen et al. 1992a). Vandenbussche et al. (2003) discuss the SEDs used for updating the Relative Spectral Response Functions (RSRF) in orbit.

The stellar calibration sources span a wide range in spectral types from A0V to M0III with the bulk of the sources being K giants. Within each of the SW AOT bands the SEDs cover more than 2 decades in flux. The diversity of the ACSs and the wide flux range increases the reliability of the photometric calibration and reduces the sensitivity to any one object or model.

As can be seen in Table 1, the star γ Dra was heavily used. The photometric calibration was checked with and without the inclusion of γ Dra to ensure this one source was not skewing the photometric calibration.

See section 6.2 for a separate discussion of the calibration of band 4.

5. PHOTOMETRIC ACCURACIES

The standard processing corrects the observed raw signal for dark current, responsivity changes (monitored with the internal calibrator), RSRF , and flat-fielding. The final step is to convert the signal at all wavelengths from instrumental units (μV/sec) to astronomical units (Jy) based on observations of

Table 1. Sources used for Photometric Calibration.

Source ID	Alias	Spectral Type	AOT Band	Number Obs.
HR7001	Vega	A0V	1&2[a]	5,0,0,0
HR2491	Sirius	A1V	1&2,3[b]	5,5,0,0
HR4534	β Leo	A3Vv	1&2	2,0,0,0
HR5459	α Cen A	G2V	-all-	1,1,1,1
HR7310	δ Dra	G9III	1&2	2,0,0,0
HR6688	ξ Dra	K2III	1&2	4,0,0,0
HR5340	α Boo	K2IIIp	-all-	8,9,9,9
HR5563	β UMi	K4III	1&2	2,0,0,0
HR1457	α Tau	K5III	-all-	6,6,6,6
HR6166	HD 149447	K5III	1&2	1,0,0,0
HR6705	γ Dra	K5III	1&2,3,3e	24,37,29,0
HR337	β And	M0III	-all-	4,4,4,2
HR911	α Cet	M2III	1&2,3,3e	2,2,2,0
HR8775	β Peg	M2.5III	3,3e,4[c]	0,7,7,7
HR4763	γ Cru	M4III	3,3e,4	0,6,6,6
NML Cyg	IRC+10448	M6IIIe	3,3e,4	0,4,3,3
Ceres	210001	Asteroid	3e,4	0,0,1,1
Uranus		Planet	3e,4	0,0,1,1

[a] 1&2 indicate bands 1A to 2C covering wavelengths from 2.4 to 12 μm. Stellar photosphere models provided by L. Decin (private communication)
[b] 3 indicates bands 3A, 3C and 3D covering wavelengths 12 to 27 μm. All Stellar photosphere composites covering 12 to 35 μm are from Cohen et al. (1992b, 1995, 1996)
[c] 3e indicates AOT band 3E (27-30 μm) and Band 4 covers the wavelength range (30-45 μm). The standard Thermal model for Ceres (T. Mueller, private communication) and the Uranus model (E. Lellouch, private communication) are obtainable from the ISO Data Centre.

Table 2. Photometric Accuracies for OLP 10.

AOT Band	Key λ μm	Bandpass μm	Accuracy 1σ %	Worst 1σ %	λ of Worst
1A	2.48	0.05	4	7	edges
1B	2.87	0.07	4	5	edges
1D	3.08	0.07	4	5	edges
1E	3.80	0.10	4	5	edges
2A	4.50	0.10	7	10	6 μm
2B	5.90	0.20	7	9	edges
2C	7.70	0.20	7	8	edges
3A	14.0	0.30	12	14	12 μm
3C	17.0	0.30	10	13	edges
3D	24.0	0.60	13	16	19.5 μm
3E	28.5	0.60	17	21	edges
4	32.0	0.60	22	23	edges

the ACSs. Table 2 lists the 1σ uncertainties in these conversion factors. As calculated, the uncertainty is the total absolute uncertainty which has accumulated factors from each of the calibration steps plus contributions from processes which were unprobed or uncorrected. Some examples of these additional uncertainties are, uncorrected memory effects in band 4, higher order memory effects in band 2, and pointing effects.

Table 2 lists the accuracies per AOT band, the key wavelength of the AOT band, the bandpass used around the key wavelength, the 1σ accuracy at the key wavelength, and the 1σ worst accuracy within the AOT band, usually at the edges of the band.

The accuracies listed in Table 2 are entirely consistent with our current knowledge of SWS and the ISO satellite. In section 6.1, the inferred pointing accuracy is on the order of 1.5-2$''$ ($1\,\sigma$). Such a large uncertainty in pointing will produce more than half of the uncertainty in photometry for bands 1 and 3 and contribute up to half of the uncertainty in bands 2 and 4.

Figures 1, 2 and 3, show 2 examples of fully calibrated spectra for α Boo and γ Cru. Each spectral segment is made up of 12 detectors. The signal from these 12 detectors is kept separate to demonstrate the flat-fielding. The SEDs for these two sources are overlaid in red. In figure 2, the up and down scans are shown separately to show the influence of residual memory effects. Figure 3 shows bands 3 and 4. In this figure radiation hits (glitches) are quite prevalent in band 4. The residual memory effect introduced by a radiation hit can artificially elevate the signal.

Also listed in the figures are the ratios of the data to the model at the key wavelength for each of the AOT bands.

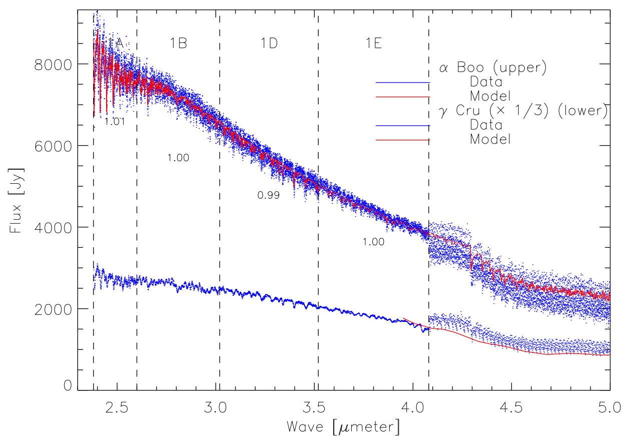

Figure 1. Band 1 for α Boo and γ Cru. Only α Boo has a full SED at these wavelengths. The SWS data are in blue and the SEDs are over-plotted in red. The data here are direct OLP 10 products without flat-fielding or rebinning.

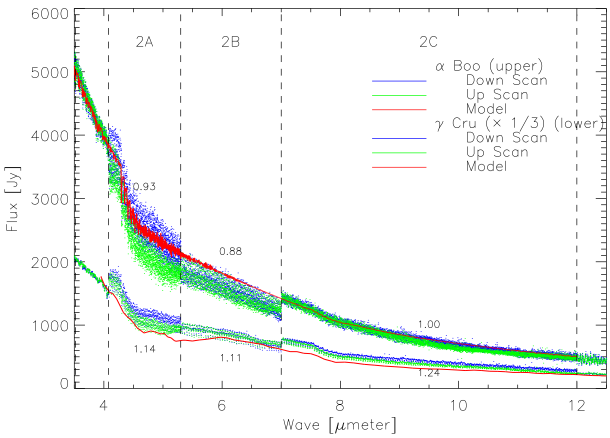

Figure 2. Band 2 for α Boo and γ Cru. Up and Down scans are shown in separate colours (blue and green) while the SEDs are shown in red. The ratio of the observation to SED is indicated. The residual memory effects are clearly seen in this figure as a mismatch between the up and the down scan. Note that the photometric calibration did not make use of the γ Cru SED for bands 1 or 2.

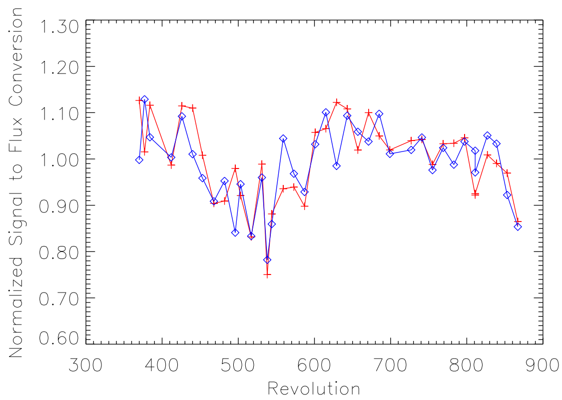

Figure 4. The photometric response to γ Dra as a function of revolution is plotted for bands 3A and 4A at the key wavelengths. The red plus signs are band 3A data and the blue diamonds are band 4A data. All 38 observations have a reconstructed pointing within 1″ of the intended coordinates. The responses have been normalised by the signal-to-flux conversion factor used for OLP 10.

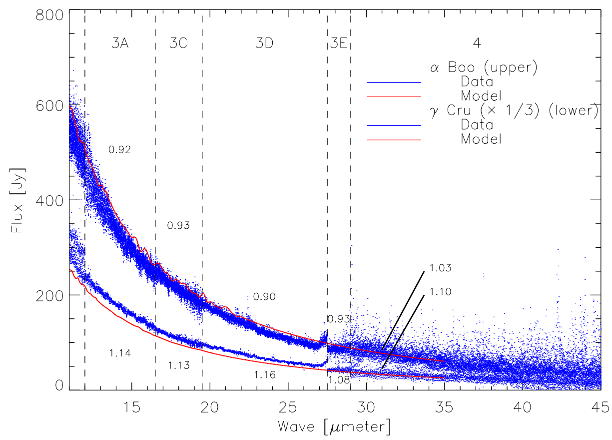

Figure 3. Bands 3 and 4 for α Boo and γ Cru. Note the extreme radiation hits in band 4 for both sources.

6. REMAINING ISSUES

6.1. INFLUENCE OF SATELLITE POINTING

The design of the SWS optics to achieve the highest spectral resolution possible, together with narrower than anticipated beam profiles (Beintema, private communication), imposed high pointing accuracies on the satellite. Although significant improvements were made throughout the mission to improve the satellite pointing (Salama 2003), there remain issues which affect the SWS photometry and the OLP10 products.

For the absolute photometric calibration, only observations with a reconstructed pointing of less than 1″ from the intended coordinates were used. Furthermore, the reconstructed pointings for observations later than revolution 451 are distributed about the intended coordinates with a 0.25″ (1σ) error. Thus according to the reconstructed pointing the majority of observations used for photometric calibration after revolution 451 should be within 0.50″ of the intended coordinates.

The most observed object for SWS was the star γ Dra. Band 3A shows time modulations in the signal of γ Dra on the order of 25%. In the same aperture as band 3A, Band 4A (non-validated off-band data) monitors the same signal from γ Dra. Figure 4 shows both bands 3A and 4A for “good” pointed observations as a function of revolution. For Band 3, the internal calibrator gain is accurate to 0.5%. For band 4, the internal calibrator is accurate to 5%. The data in 4 have been corrected for any detector variation. A responsivity variation of 20% by the SWS instrument would have been seen and corrected by the pipeline processing. Given this fact, and the fact that two separate detector blocks see the same variation, the indication is that the source of the modulation is outside of SWS. The simplest means of producing the signal variation is through satellite (mis)pointings.

Analysis of the SWS beam profiles indicates that a 2″ variation in pointing is needed to produce the observed trend in Figure 4. This conclusion is at odds with the reconstructed pointing accuracy of 0.5″. Despite the significant efforts of a number of people, no pointing solution has yet been found and the mismatch of SWS data and reconstructed pointing data remains an issue.

There is an indication that the trend shown in Figure 4 occurs for other calibration sources as well. However, in the final OLP10 photometric calibration, a correction for this variation was not introduced for two reasons. First, without a pointing model which reproduces the observed 2″ trend, the evidence that the same trend applies **uniformly** over the sky is too weak. Secondly, objects extended to the SWS beam would be adversely affected by a photometric calibration which caters to a point-source-specific problem.

Through the same mechanism as the signal modulation above, the pointing also influences the ability to match up AOT bands in their overlap regions. Thus full SWS grating scans often have unrealistic discontinuities between AOT bands whereas the data within an AOT band seem very stable and continuous. These jumps are especially noticeable between aperture changes.

The SWS observations strongly suggest that there remains a pointing error (either systematic or random) on the order of $2''$. These errors are carried into the photometric uncertainties listed in Table 2 and are discussed in that section.

6.2. Calibrating Band 4

Band 4 suffers from a number of problems. As can be seen from Figure 3, radiation hits reduce the sensitivity of this band and complicate the photometry on low signal sources. Furthermore, the RSRF for band 4 relies entirely on laboratory observations without the benefit of an in-orbit update. The laboratory RSRF was calculated from a very bright, completely extended source. Therefore, memory effects and some non-linearities come into play in the ground based data for the RSRF. Through the RSRF, these problems may be carried into the science observations as well.

7. CONCLUSIONS

This article presented an overview of the calibration of the Short Wavelength Spectrometer grating at the end of the ISO post operations phase. Both the spectroscopic and photometric calibration and accuracies are reasonably well understood and within pre-launch requirements. SWS benefited from both excellent planning and hard work. The instrument was well monitored and, when necessary, the calibration was allowed to evolve.

The main sources of uncertainties in the photometric calibration of SWS are memory effects, pointing effects and calibration sources (especially at the longer wavelengths). The most pressing topic for calibration is the improvement of Band 4. This work is currently being planned.

ACKNOWLEDGEMENTS

The authors would like to thank Leen Decin, Thomas Mueller and Emmanuel Lellouch for kindly providing some of the model SEDs used for photometric calibration. RFS would like to thank Leen Decin for many useful discussions.

REFERENCES

Cohen, M., Walker, R.G., & Witteborn, F.C., 1992a, AJ, 104, 2030
Cohen, M., Walker, R.G., Barlow, M.J., & Deacon, J.R., 1992b, AJ, 104, 1650
Cohen, M., Witteborn, F.C., Walker, R.G., Bregman, J., & Wooden, D.H., 1995, AJ, 110, 275
Cohen, M., Witteborn, F.C., Carbon, D.F., Davies, J.K., Wooden, D.H., & Bregman, J., 1996, AJ, 112, 2274
Decin, L., 2000, PhD. Thesis, Katholieke Universiteit Leuven
Fouks, B.I., & Schubert, J., 1995, SPIE, 2475, 487
de Graauw, Th. et al., 1996, A&A , 315, L49
Heras, A. et al., 2000, Exp. Astronomy, 10, 177
Kester, D., Beintema, D. & Valentijn, E., 1998, SWS Technical Report, "SWS Grating Wavelength Calibration"
Kester, D., 2001, SWS Technical Report, "Memory Effects and their Correction in SWS Si:Ga Detectors"
Lorente, R., 1998, SWS Technical Report, "Spectral Resolution of SWS AOT1"
Lutz, D., Feuchtgruber, H., and Morfill, J., 1999, SWS Technical Report MPE-ISO-99-1, "ISO-SWS grating resolution and instrumental profile as measured by the full resolution modes SWS02 and SWS06"
Salama, A., 2003, this volume
Schaeidt, S.G. et al., 1996, A&A, 315, L55
Shipman, R.F., 2000, SWS Technical Report, "Testing of SWS Flatfield"
Shipman, R.F. & Lahuis, F., 2000, SWS Technical Report, "Modification of SWS Flux Calibration"
Valentijn, E.A. et al., 1996, A&A, 315, L60
Valentijn, E.A., Lutz. D., & Salama. A., 1995, SWS Technical Report ISO-94-23, "In Orbit Calibration Document"
Vandenbussche, B. et al., 2003, this volume